Enhancement of the Wave Energy Conversion Characteristics of a Hinge-Barge Using Pseudospectral Control

Francesco Paparella
Centre for Ocean Energy Research (COER)
Maynooth University
Co. Kildare, Ireland
Email: francesco.paparella.2014@mumail.ie

John V. Ringwood
Centre for Ocean Energy Research (COER)
Maynooth University
Co. Kildare, Ireland
Email: john.ringwood@eeng.nuim.ie

***Abstract*—This paper shows the benefits of using pseudo-spectral (PS) methods for the optimal control of a three-body hinge-barge device. Two different control formulations are derived based on different representations of the dynamic model of the device: the differential and algebraic equations (DAE) formulation, and the ordinary differential equations (ODE) formulation. Wave-tank tests are carried out in order to validate the DAE and ODE models against experimental data. For control design, PS methods show significant improvements in terms of absorbed power with respect to an optimal damping strategy.**

I. Introduction

Hinge-barge wave energy converters are articulated floating structures that extract energy carried by the waves. The hinge-barge device as shown in Figure 1 is composed of a number of rectangular bodies interconnected by hinges, and is considered to be an attenuator device, since it operates longitudinally to the direction to the incoming wave. The relative pitch motion between each pair of bodies is used to drive a Power Take Off (PTO) system. Examples of hinge-barge WECs include the McCabe Wave Pump (MWP) [1] and the SeaPower Platform [2]. Another example of an articulated WEC is the Pelamis WEC which is composed of multiple cylindrical section linked by hinged joints [3]. For the Pelamis WEC, the control of the power absorbed at each joint axis is realized considering the inputs from all axes. Therefore, the real-time control of all forces is implemented with respect to the entire machine response. However, little detail on the control strategies for the Pelamis WEC is provided in the available literature. In [4], a hinged 5-body WEC consisting of a circular center floater hinged to 4 smaller spherical buoys is considered. The relative rotation between the central body and each buoy is used to drive a PTO, and the absorbed energy is maximized for both regular and irregular waves. For regular waves, the optimal velocities and control forces are computed at each frequency of the incident wave for both passive and active control. A passive PTO is able to absorb energy from the device only, while an active PTO can also deliver power from the grid to the device. The optimization of the damping coefficients of passive PTOs is also considered for the regular wave case. For irregular waves, only the optimization of frequency-independent damping coefficients of passive PTOs is considered for waves represented by different realizations of the JONSWAP spectrum [5]. In this paper, both passive and active controllers, which compute the optimal profile of velocities and control forces of the PTOs, are considered for both regular and irregular waves. The objective of this paper is to asses the value of optimal pseudo-spectral (PS) control methods applied to a three-body hinge-barge wave energy device. PS methods are a subset of the class of techniques used for the discretisation of integral and partial differential equations known as mean weighted residuals [6], [7]. In [8], PS methods are applied for the optimal control of generic WECs. The remainder of the paper is organized as follows: In Section II, the dynamic model of a three-body hinge-barge device is derived while, in Section III, PS methods are applied to solve the dynamics of a three-body hinge-barge device. In section IV, the dynamic model of the device is compared against tank test data to verify its validity while, in Section V, PS methods are applied to optimally control a three-body hinge-barge device. In Section VI, PS optimal control is compared to a standard optimal controller for both monochromatic and polychromatic waves. Finally, overall conclusions are drawn in Section VII.

II. Dynamic model of a three-body hinge-barge device

This section briefly describes the dynamic model of a three-body hinge-barge device originally derived in [9]. In Figure 1, the device is represented together with the global frame X_g, Z_g, while a body frame is assigned to each body composing the device. The analysis of the motion of the devices is restricted to the two dimensional plane $X-Z$. The total number of independent degrees of freedom of the system in Figure 1 is four: The heave displacement z_2 of body 2, and the pitch angles θ_1, θ_2 and θ_3 of bodies 1, 2 and 3, respectively.

The dynamic model of the device can be derived with two different formulations: the Differential and Algebraic Equations (DAE) formulation and the Ordinary Differential

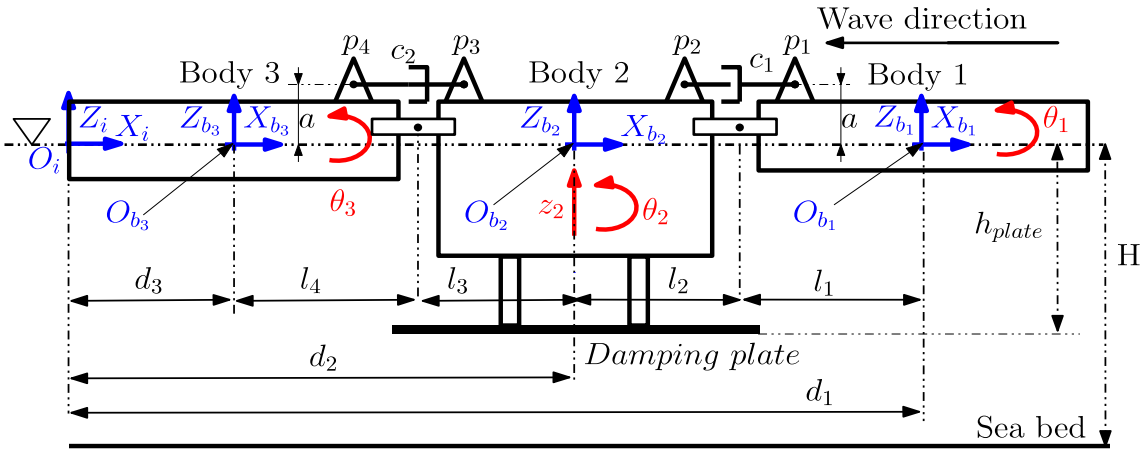

Fig. 1. Three-body hinge-barge device, where $X_g Z_g$ represents the global frame, and a local frame is assigned to each body composing the device.

Equations (ODE) formulation. In the DAE formulation, the model is described as a set of differential equations for the generalized coordinates of the unconstrained system and the constraints are described by algebraic equations. In the ODE formulation, the constraint equations are no longer described explicitly, but rather embedded into a set of differential equations for the independent degrees of freedom of the system only.

A. DAE formulation

In this subsection, the DAE formulation is applied in order to obtain the equations of motion for a three-body hinge-barge device. The equations of motion are given as follows [9]:

$$\dot{\mathbf{q}} = \mathbf{J}(\boldsymbol{\Theta})\mathbf{v} \tag{1}$$

$$\mathbf{M}\dot{\mathbf{v}} + (\mathbf{B} + \mathbf{B}_{visc})\mathbf{v} + \mathbf{C}_z^T \boldsymbol{\lambda} = -\mathbf{G}\mathbf{q} - \mathbf{M}_\infty \dot{\mathbf{v}} + .. - \int_{-\infty}^{t} \mathbf{K}_{rad}(t-\tau)\mathbf{v}, d\tau + \mathbf{f}_{wave} + \mathbf{f}_{PTO} \tag{2}$$

$$\mathbf{C}(\mathbf{z}, t) = 0 \tag{3}$$

where $\mathbf{z}$ is the vector of generalized positions expressed in the body frame of each body:

$$\mathbf{z} = [\mathbf{z}_1\ \mathbf{z}_2\ \mathbf{z}_3]^T = [z^b_{i,b_1}\ \theta_1\ z^b_{i,b_2}\ \theta_2\ z^b_{i,b_3}\ \theta_3]^T \tag{4}$$

where z^b_{i,b_k} and θ_k are the heave displacement and pitch angle of body k, respectively, with $k = 1, 2, 3$. The vector $\mathbf{v}$ represents the generalized velocities expressed in the body frame of each body, while the vector $\mathbf{q}$ represents the generalized positions expressed in the global frame. The transformation matrix $\mathbf{J}(\boldsymbol{\Theta})$ and the rigid-body inertia matrix $\mathbf{M}$ in equation (2) are described in [10]. The terms $\mathbf{B}$ and $\mathbf{B}_{visc}$ in equation (2) represent the coriolis-centripetal and viscous matrix, respectively. The hydrodynamic loads $\mathbf{G}$, $\mathbf{M}_\infty$, $\mathbf{K}_{rad}$ and $\mathbf{f}_{wave}$ in equation (2) are obtained by means of the boundary element software WAMIT [11]. The vector $\boldsymbol{\lambda}$ represents the constraint forces. The vector of PTO forces $\mathbf{f}_{PTO}$ in equation (2) is given by the forces due to the PTO systems connecting body 2 to bodies 1 and 3. As shown in Figure 1, each PTO component is represented as a linear dash-pot system. The vector of loads, due to the PTO systems acting on the device, is given as follows:

$$\mathbf{f}_{PTO} = -\begin{bmatrix} 0 & -F_{s1}a & 0 & F_{s1}a - F_{s2}a & 0 & F_{s2}a \end{bmatrix}^T \tag{5}$$

where:

$$F_{s1} = c_1 \dot{l}_1 \tag{6}$$

$$F_{s2} = c_2 \dot{l}_2 \tag{7}$$

where c_i, l_i, with $i = 1, 2$, are the damping coefficients and length of the dash-pot system connecting body 2 to body 1 and 3, respectively. Now, the constraint equations $\mathbf{C}(\mathbf{z}, t)$ in equation (3) are derived in [9], and the matrix of the partial derivatives of constraint equations, computed with respect to the generalized positions and linearized around the equilibrium position, is given as follows:

$$\mathbf{C}_z = \begin{bmatrix} 0 & 0 & 1 & -l_3 & -1 & -l_4 \\ 1 & -l_1 & -1 & -l_2 & 0 & 0 \end{bmatrix} \tag{8}$$

B. ODE formulation

The ODE formulation is now applied to obtain the equations of motion of a three-body hinge-barge device. The vector of independent velocities of the device is:

$$\mathbf{v}_s = [\dot{\theta}_1\ \dot{z}^b_{i,b_2}\ \ \dot{\theta}_2\ \dot{\theta}_3]^T \tag{9}$$

Given the matrix $\mathbf{C}_z$ from equation (8), the transformation matrix $\mathbf{P}$ used to express the relation between the vector of generalized velocities and independent velocities is given as follows:

$$\mathbf{P} = \begin{bmatrix} l_1 & 1 & l_2 & 0 \\ 1 & 0 & 0 & 0 \\ 0 & 1 & 0 & 0 \\ 0 & 0 & 1 & 0 \\ 0 & 1 & -l_3 & -l_4 \\ 0 & 0 & 0 & 1 \end{bmatrix} \tag{10}$$

Using $\mathbf{P}$, the equations of motion of the device expressed with respect to the independent degrees of freedom are given as follows:

$$\dot{\mathbf{q}}_s = \mathbf{v}_s \tag{11}$$

$$\mathbf{M}_s\dot{\mathbf{v}}_s + (\mathbf{B}_s + \mathbf{B}_{visc,s})\mathbf{v}_s = -\mathbf{G}_s\mathbf{q}_s - \mathbf{M}_{\infty,s}\dot{\mathbf{v}}_s + .. - \int_{-\infty}^{t} \mathbf{K}_{rad,s}(t-\tau)\mathbf{v}_s, d\tau + \mathbf{f}_{wave,s} + \mathbf{f}_{PTO,s} \tag{12}$$

where:

$$\mathbf{M}_s = \mathbf{P}^T\mathbf{M}\mathbf{P} \tag{13}$$
$$\mathbf{B}_s = \mathbf{P}^T\mathbf{B}\mathbf{P} + \mathbf{P}^T\mathbf{M}\dot{\mathbf{P}} + \mathbf{P}^T\mathbf{M}_\infty\dot{\mathbf{P}} \tag{14}$$
$$\mathbf{B}_{visc,s} = \mathbf{P}^T\mathbf{B}_{visc}\mathbf{P} \tag{15}$$
$$\mathbf{G}_s = \mathbf{P}^T\mathbf{G}\mathbf{P} \tag{16}$$
$$\mathbf{M}_{\infty,s} = \mathbf{P}^T\mathbf{M}_\infty\mathbf{P} \tag{17}$$
$$\mathbf{K}_{rad,s} = \mathbf{P}^T\mathbf{K}_{rad}\mathbf{P} \tag{18}$$
$$\mathbf{f}_{wave,s} = \mathbf{P}^T\mathbf{f}_{wave} \tag{19}$$
$$\mathbf{f}_{PTO,s} = \mathbf{P}^T\mathbf{f}_{PTO} \tag{20}$$

III. Pseudo-spectral approximation methods

In this section, PS methods are used to compute an approximate solution to the integro-differential equations obtained for the DAE and ODE formulations. Given the periodic nature of the variables associated with the problem, positions and velocities that appear in the equations of motion obtained for the DAE and ODE formulations can be approximated with a linear combination of zero mean trigonometric polynomials (truncated Fourier series) as follows:

$$\begin{aligned} q_i(t) \approx q_i^M(t) &= \sum_{k=1}^{M} x_{i,k}^{q,c} cos(k\omega_0 t) + x_{i,k}^{q,s} sin(k\omega_0 t) \\ &= \mathbf{\Phi}(t)\hat{\mathbf{x}}_i^q \end{aligned} \tag{21}$$

$$\begin{aligned} v_i(t) \approx v_i^M(t) &= \sum_{k=1}^{M} x_{i,k}^{v,c} cos(k\omega_0 t) + x_{i,k}^{v,s} sin(k\omega_0 t) \\ &= \mathbf{\Phi}(t)\hat{\mathbf{x}}_i^v \end{aligned} \tag{22}$$

where $i = 1, .., 6N$ and $i = 1, .., n$ for the DAE and ODE formulations, respectively. The parameter M is the order of expansion for the positions and velocities. The vector of the coefficients $\hat{\mathbf{x}}_i^q$ and $\hat{\mathbf{x}}_i^v$ of the approximated components of the position and velocity vectors, are given as follows:

$$\hat{\mathbf{x}}_i^q = \begin{bmatrix} x_{i,1}^{q,c} & x_{i,1}^{q,s} & .. & x_{i,M}^{q,c} & x_{i,M}^{q,s} \end{bmatrix}^T \tag{23}$$

$$\hat{\mathbf{x}}_i^v = \begin{bmatrix} x_{i,1}^{v,c} & x_{i,1}^{v,s} & .. & x_{i,M}^{v,c} & x_{i,M}^{v,s} \end{bmatrix}^T \tag{24}$$

while the basis function vector $\mathbf{\Phi}(t)$ is given as follows:

$$\mathbf{\Phi}(t) = \begin{bmatrix} cos(\omega_0 t) & sin(\omega_0 t) & .. & cos\,(M\omega_0 t) & sin\,(M\omega_0 t) \end{bmatrix}^T \tag{25}$$

where $\omega_0 = 2\pi/T_0$ is the fundamental frequency. The derivatives of the ith components of the position and velocity vector are, respectively,

$$\dot{q}_i^M(t) = \dot{\mathbf{\Phi}}(t)^T\hat{\mathbf{x}}_i^q = \mathbf{\Phi}(t)^T\mathbf{D}_\phi\hat{\mathbf{x}}_i^q \tag{26}$$
$$\dot{v}_i^M(t) = \dot{\mathbf{\Phi}}(t)^T\hat{\mathbf{x}}_i^v = \mathbf{\Phi}(t)^T\mathbf{D}_\phi\hat{\mathbf{x}}_i^v \tag{27}$$

where $\mathbf{D}_\phi \in \mathbb{R}^{2M\times 2M}$ is a block diagonal matrix, with the k-th block ($k = 1, .., M$) given as follows:

$$\mathbf{D}_{\phi,k} = \begin{bmatrix} 0 & k\omega_0 \\ -k\omega_0 & 0 \end{bmatrix} \tag{28}$$

Regarding the DAE formulation, substituting the approximated states (21), (22) and their time derivatives (26), (27) into the equations of motion (1)-(3) yields the following equations of motion in residual form:

$$r_i^q(t) = \mathbf{\Phi}(t)\mathbf{D}_\phi\hat{\mathbf{x}}_i^q - \sum_{p=1}^{6N} J_{i,p}\mathbf{\Phi}(t)\hat{\mathbf{x}}_p^v \tag{29}$$

$$\begin{aligned} r_i^v(t) = &\sum_{p=1}^{6N} M_{i,p}\mathbf{\Phi}(t)\mathbf{D}_\phi\hat{\mathbf{x}}_p^v + \sum_{p=1}^{6N} B_{i,p}\mathbf{\Phi}(t)\hat{\mathbf{x}}_p^v + \sum_{p=1}^{6N} G_{i,p}\mathbf{\Phi}(t)\hat{\mathbf{x}}_p^q \\ &+ \sum_{p=1}^{6N}\int_{-\infty}^{t} K_{rad_{i,p}}(t-\tau)\mathbf{\Phi}(\tau)\hat{\mathbf{x}}_p^v d\tau + \sum_{p=1}^{m} C_{q_{i,p}}^T\mathbf{\Phi}(t)\hat{\mathbf{x}}_p^\lambda(t) \\ &- f_{wave,i}(t) - f_{pto,i}(t) \end{aligned} \tag{30}$$

$$r_j^C(t) = C_j(\mathbf{q}, t) \tag{31}$$

where $i = 1, .., 6N$, $j = 1, .., m$, and $J_{i,p}$, $M_{i,p}$, $B_{i,p}$, $G_{i,p}$, $K_{rad_{i,p}}$ and $C_{q_{i,pp}}^T$ are the elements of the matrices $\mathbf{J}(\mathbf{\Theta})$, $\mathbf{M}$, $\mathbf{B}$, $\mathbf{G}$, $\mathbf{K}_{rad}$ and $\mathbf{C}_q^T$, respectively.

Regarding the ODE formulation, substituting the approximated states (21), (22) and their time derivatives (26), (27) into the equations of motion (11)-(12), yields:

$$r_i^q(t) = \mathbf{\Phi}(t)\mathbf{D}_\phi\hat{\mathbf{x}}_i^q - \mathbf{\Phi}(t)\hat{\mathbf{x}}_i^v \tag{32}$$

$$\begin{aligned} r_i^v(t) = &\sum_{p=1}^{n} M_{s_{i,p}}\mathbf{\Phi}(t)\mathbf{D}_\phi\hat{\mathbf{x}}_p^v(t) + \sum_{p=1}^{n} B_{s_{i,p}}\mathbf{\Phi}(t)\hat{\mathbf{x}}_p^v \\ &+ \sum_{p=1}^{n} G_{s_{i,p}}\mathbf{\Phi}(t)\hat{\mathbf{x}}_p^q + \sum_{p=1}^{n}\int_{-\infty}^{t} K_{rad,s_{i,p}}(t-\tau)\mathbf{\Phi}(\tau)\hat{\mathbf{x}}_p^v d\tau \\ &- f_{wave,s_i}(t) - f_{pto,s_i}(t) \end{aligned} \tag{33}$$

where $i = 1, .., n$, and $M_{s_{i,p}}$, $B_{s_{i,p}}$, $G_{s_{i,p}}$ and $K_{rad,s_{i,p}}$ are the elements of the matrices $\mathbf{M}_s$, $\mathbf{B}_s$, $\mathbf{G}_s$ and $\mathbf{K}_{rad,s}$, respectively. PS methods are used to compute the coefficients $\hat{\mathbf{x}}_i^q$ and $\hat{\mathbf{x}}_i^v$ that minimize the residuals (29)-(31) and (32)-(33) for the DAE and ODE formulations, respectively [12].

IV. Model validation

The purpose of this section is to identify and validate the dynamic model of the hinge-barge device against tank experiments. The optimization of the WEC geometry is beyond the scope of this paper. A specific three-body hinge-barge device was tested in a wave tank using facilities of the U.S. Naval Academy, Annapolis [13]. The dimensions of body 1 are: length= 0.68 m, width=0.4 m and height=0.1 m. The dimensions of body 2 are: length= 0.28 m, width=0.4 m and height=0.15m. The dimensions of body 3 are: length= 1 m, width=0.4 m and height=0.1 m. The PTO is made of two dashpots placed above the hinges and connecting body 2 to body 1 and 3, as shown in Figure 1. A tank test with an incident wave from a Bretschneider spectrum with a significant wave height $H_s = 15$ cm and significant period $T = 1.276$ seconds was performed, with the direction of the waves along the longitudinal direction of the device. Given the frequency domain model of the device, the viscous damping matrix $\mathbf{B}_{visc,s}$ and the phases of the vector of the excitation forces $\mathbf{f}_{wave,s}$ in equation (12) can be identified using the irregular wave test [9]. To validate the identified model, a series of tank tests with an incident wave from a Jonswap spectrum with a significant wave height $H_s = 15$ cm and significant period $T = 1.276$ seconds was performed. PS methods were applied to compute an approximate solution for the equations of motion obtained for the DAE and ODE formulations. A fundamental frequency $\omega_0 = 0.12$ rad/s is chosen, while the order of expansion N_x for the position and velocity of the states is 70. Note that the response of the device obtained with the ODE and DAE formulations are identical. In Figure 2, the frequency response of the heave of body 2 obtained from the tank experiments is compared against the response obtained from the ODE formulation. In Figure 3, the frequency responses of the pitch angles of bodies 1,2 and 3 obtained from the tank experiments are compared against the responses obtained from the ODE formulation. In Figure 4, the time domain response of the heave of body 2 obtained from the tank experiments is compared against the response obtained from the ODE formulation. In Figure 5, the time domain responses of the pitch angles of bodies 1,2 and 3 obtained from the tank experiments are compared against the responses obtained from the ODE formulation. Both DAE and ODE PS formulations showed good agreement with experimental tests in terms of device motion.

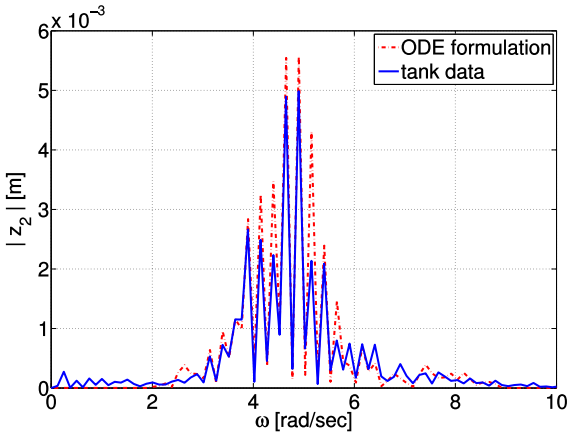

Fig. 2. Frequency response of the heave of body 2 obtained from tank experiments and ODE formulation for an irregular wave made using using Jonswap spectrum with a significant wave height $H_s = 15$ cm and significant period $T = 1.276$ sec.

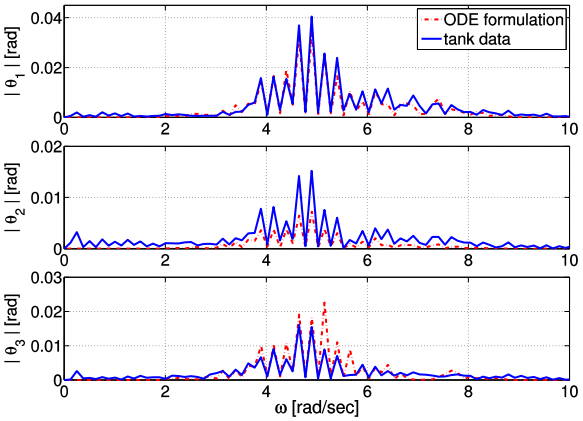

Fig. 3. Frequency response of the pitch angles of body 1, 2 and 3 obtained from tank experiments and ODE formulation for an irregular wave made using using Jonswap spectrum with a significant wave height $H_s = 15$ cm and significant period $T = 1.276$ sec.

V. Pseudo-spectral optimal WEC control

This section describes the direct transcription of the optimal control problem [8] for a three-body hinge barge device. For a generic WEC control problem, the vector of PTO forces in equation (2) is considered to be $\mathbf{f}_{PTO} = \mathbf{F}_p\mathbf{u}$, where $\mathbf{F}_p$ is the configuration matrix and $\mathbf{u}$ is the vector of control variables [8]. For the case of a three-body hinge-barge device, $\mathbf{F}_p$ is given as:

$$\mathbf{F}_p = \begin{bmatrix} 0 & 1 & 0 & -1 & 0 & 0 \\ 0 & 0 & 0 & -1 & 0 & 1 \end{bmatrix}^T \tag{34}$$

and the vector of control variables is considered to be $\mathbf{u} = [\tau_1 \ \tau_2]^T$, where τ_1 is the torque applied by the PTO connecting body 2 and 1, while τ_2 is the torque applied by the PTO connecting body 2 and 3. The torques can be approximated as follows:

$$\begin{aligned} \tau_p(t) \approx \tau_p^M(t) &= \sum_{k=1}^{M} u_{p,k}^c cos(k\omega_0 t) + u_{p,k}^s sin(k\omega_0 t) \\ &= \mathbf{\Phi}(t)\hat{\mathbf{u}}_p \end{aligned} \tag{35}$$

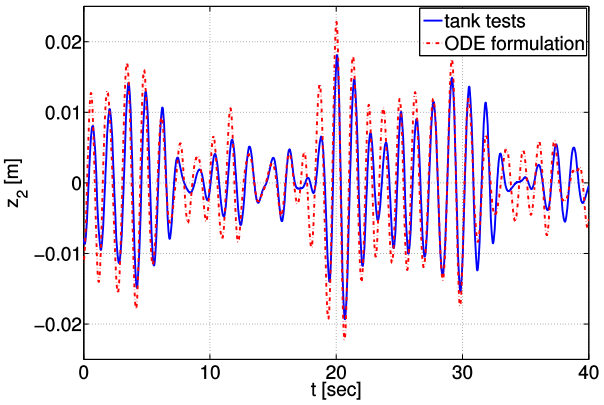

Fig. 4. time domain response of the heave of body 2 obtained from tank experiments and ODE formulation for an irregular wave made using using Jonswap spectrum with a significant wave height $H_s = 15$ cm and significant period $T = 1.276$ sec.

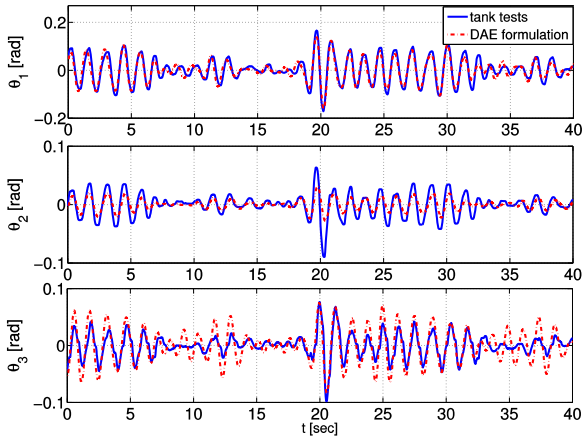

Fig. 5. time domain response of the pitch angles of body 1, 2 and 3 obtained from tank experiments and ODE formulation for an irregular wave made using using Jonswap spectrum with a significant wave height $H_s = 15$ cm and significant period $T = 1.276$ sec.

with $p = 1, 2$. The vector of the coefficients $\hat{\mathbf{u}}_p$ is given as follows:

$$\hat{\mathbf{u}}_p = \left[u^c_{p,1}\ u^s_{p,1}\ ..\ u^c_{p,N_u}\ u^s_{p,M}\right]^T \tag{36}$$

The cost function considered for the optimal control problem is as follows:

$$J = \frac{1}{T}\int_0^T (\mathbf{v}^T\mathbf{F}_p\mathbf{u} - r\mathbf{u}^T\mathbf{u})dt \tag{37}$$

where r is a weighting parameter. The cost function in equation (37) balances the average power absorbed by the PTOs and the squared norm of the control vector using the parameter r. The term $r\mathbf{u}^T\mathbf{u}$ in equation (37) is used to ensure a convex cost function which facilitates the search of the globally optimal solution to the optimization problem. By substituting the approximated velocities and control torques defined in equations (22) and (35), respectively, into equation (37), the cost function can be written as:

$$\begin{aligned} J^M &= \frac{1}{T}\int_0^T \mathbf{\Phi}(t)^T(\ \mathbf{X}^V\mathbf{F}_p\mathbf{U}^T - r\mathbf{U}\mathbf{U}^T)\ \mathbf{\Phi}(t)dt \\ &= \frac{1}{2}(\ \hat{\mathbf{u}}_1^T(\hat{\mathbf{x}}_2^v - \hat{\mathbf{x}}_4^v) + \hat{\mathbf{u}}_2^T(\hat{\mathbf{x}}_6^v - \hat{\mathbf{x}}_4^v) - r(\ \hat{\mathbf{u}}_1^T\hat{\mathbf{u}}_1 + \hat{\mathbf{u}}_2^T\hat{\mathbf{u}}_2)\ ) \\ &= \frac{1}{2}\mathbf{x}^T\mathbf{H}\mathbf{x} \end{aligned}$$

where: (38)

$$\mathbf{X}^V = [\ \hat{\mathbf{x}}_1^v, .., \hat{\mathbf{x}}_n^v] \tag{39}$$

$$\mathbf{U} = [\ \hat{\mathbf{u}}_1\ \ \hat{\mathbf{u}}_2] \tag{40}$$

$$\mathbf{H} = \begin{bmatrix} \mathbf{0}_{6\times 2M} & \mathbf{0}_{6\times 2M} & \mathbf{0}_{2\times 2M} \\ \mathbf{0}_{6\times 2M} & \mathbf{0}_{6\times 2M} & \mathbf{H}_1 \\ \mathbf{0}_{2\times 2M} & \mathbf{H}_2 & \mathbf{I}_{2\times 2M} \end{bmatrix} \tag{41}$$

$$\mathbf{H}_1 = \begin{bmatrix} \mathbf{0}_{2M} & \mathbf{0}_{2M} \\ \mathbf{I}_{2M} & \mathbf{0}_{2M} \\ \mathbf{0}_{2M} & \mathbf{0}_{2M} \\ -\mathbf{I}_{2M} & -\mathbf{I}_{2M} \\ \mathbf{0}_{2M} & \mathbf{0}_{2M} \\ \mathbf{0}_{2M} & \mathbf{I}_{2M} \end{bmatrix} \tag{42}$$

$$\mathbf{H}_2 = \mathbf{H}_1^T \tag{43}$$

where $\mathbf{0}_k$ is a square matrix of zeros of dimension k and $\mathbf{I}_k$ is an identity matrix of dimension k. Therefore, the optimal control problem is defined by a finite dimensional optimization problem with cost function (38), and dynamic constraints (29)-(31) and (32)-(33) for the DAE and ODE formulations, respectively.

VI. Control Results

In this section, PS methods are applied to control a three-body hinge-barge device, given the model in Section IV.

A. Regular waves

The power dissipated by the PTO systems was recorded for a series of regular wave tests performed for a range of frequencies ω from 3.14 rad/sec to 7.54 rad/secs and direction of the waves along the longitudinal direction of the device. In Figure 6, the dynamic model shows a good agreement with the tank data in terms of capture width ratio. An alternative strategy to PS methods for the control of the device is to consider a model in the frequency domain, and compute the optimal linear damping coefficients of the PTOs that maximizes the energy absorption at each frequency of the incoming wave [14]. In Figure 6, a comparison between the capture width ratio given by the optimal linear damping control, PS passive and active control is evaluated for each frequency of the regular incoming wave. For the PS active and passive control, the fundamental frequency ω_0 of positions, velocities and torques is equal to the frequency of the incoming wave, while the order of expansion N_x is equal to 1. A convex cost function, defined as in equation (38) with $r = 10$, is considered for both PS passive and active control.

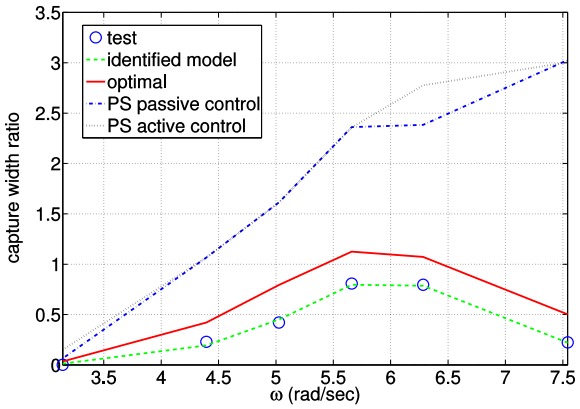

Fig. 6. Comparison between the capture width ratio given by the tank data, dynamic model, optimal linear damping control, PS passive control and PS active control with convex cost function for different frequencies of a regular wave of amplitude $A = 2$ cm.

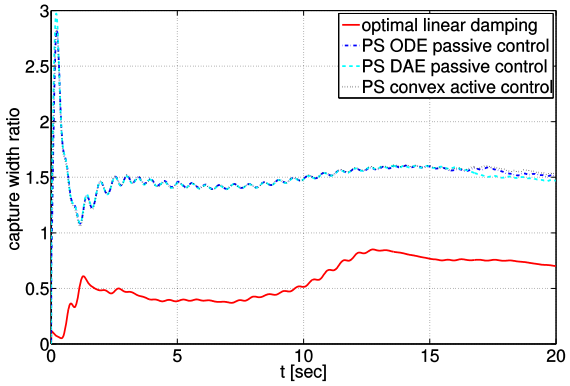

Fig. 7. Time domain comparison of the capture width ratio given by the hinge-barge device with optimal linear damping control, PS ODE and DAE passive control and PS active control with convex cost function for a polychromatic wave made using JONSWAP spectrum with a significant wave height $H_s = 15$ cm and significant period $T = 1.276$ secs.

B. Irregular waves

In Figure 7, a comparison between the capture width ratio with the optimal linear damping control, PS ODE and DAE passive control, and PS active control with convex cost function is shown for a polychromatic wave over a time horizon of 20 s. For the PS active and passive control, the fundamental frequency of positions, velocities and torques is equal to $\omega_0 = 0.314$ rad/s, while the order of expansion N_x is equal to 30. The polychromatic wave is obtained from a JONSWAP spectrum with a significant wave height $H_s = 15$ cm and significant period $T = 1.276$ secs. It is important to highlight that a trade-off value for r that ensures the convexity of the cost function without degrading the absorbed power significantly must be selected appropriately for each time horizon of the control problem. This is consistent with the use of Model Predictive Control (MPC) for wave energy conversion control problems [15].

VII. Conclusions

This paper demonstrates that PS methods are a compact and efficient formulation for the modelling and control of a three-body hinge-barge device. Experimental tests on a specific three-body hinge-barge device with polychromatic waves were carried out to validate the use of the PS models. Both DAE and ODE PS formulations showed good agreement with experimental tests in terms of device motion. Furthermore, this paper shows that, for regular and irregular waves, the average absorbed power with both PS passive and active control is approximately two times greater than the average absorbed power with optimal linear passive dampers.

Acknowledgment

This paper is based upon works supported by the Science Foundation Ireland under Grant No. 12/RC/2302 for the Marine Renewable Ireland (MaREI) centre. The authors wish to acknowledge Andrew Paulmeno and Sarah E. Mouring from the U.S. Naval Academy for providing the data for the validation of the hinge-barge model.

References

[1] Falcão, A., "Wave energy utilization: A review of the technologies," *Renewable and Sustainable Energy Reviews*, vol. 14, no. 3, pp. 899–918, 2010.

[2] Sea Power Ltd. Available from: http://www.seapower.ie.

[3] Yemm, R., Pizer, D., Retzler, C., and Henderson, R., "Pelamis: experience from concept to connection," *Philosophical Transactions of the Royal Society A*, vol. 370, pp. 365–380, 2012.

[4] Øyvind Ygre Rogne, "Numerical and experimental investigation of a hinged 5-body wave energy converter," Ph.D. dissertation, Norwegian University of Science and Technology, Faculty of Engineering Science and Technology, Department of Marine Technology, 2014.

[5] M. K. Ochi, *Ocean Waves, The Stochastic Approach*. Cambridge University Press, 1998.

[6] Canuto, C., Hussaini, Y., Quarteroni, A., and Zang, T., *Spectral Methods: Fundamentals in Single Domains*. Springer, 2006.

[7] Fornberg, B., *A Practical Guide to Pseudospectral Methods*. Cambridge University Press, 1996.

[8] Bacelli, G. and Ringwood, J.V., "Numerical optimal control of wave energy converters," *IEEE Transactions on Sustainable Energy*, vol. 6, no. 2, pp. 294–302, 2015.

[9] Paparella, F., Bacelli, G., Paulmeno, A., Mouring, S. E., and Ringwood, J.V., "Multi-body modelling of wave energy converters using pseudo-spectral methods with application to a three-body hinge-barge device," *IEEE Transactions on Sustainable Energy*, In press.

[10] Fossen, T. I., *Handbook of marine craft hydrodynamics and motion control*. Wiley, 2011.

[11] *WAMIT User Manual Version 7.0*, Massachusetts Institute of Technology, USA.

[12] Elnagar, G., Kazemi, M. A., and Razzaghi, M., "The pseudospectral Legendre method for discretizing optimal control problems," *IEEE Transactions on Automatic Control*, vol. 40, no. 10, 1995.

[13] Paulmeno, A., "An Experimental Analysis of the Optimal Design Conditions for a Model Scale McCabe Wave Pump," Department of Naval Architecture and Ocean Engineering, United States Naval Academy Annapolis, Maryland 21402, Independent Research in Ocean Engineering Honors Final Report, May 2013.

[14] J. Falnes, *Ocean Waves and Oscillating Systems*. Cambridge, U.K.: Cambridge University Press, 2002.

[15] Li, G. and Belmont, M.R., "Model predictive control of sea wave energy converters - Part I: A convex approach for the case of a single device," *Renewable Energy*, vol. 69, pp. 453–463, 2014.